

conferenza **Att** Proceedings

Building Simulation Applications BSA 2015

2nd BPSA Italy conference

Bozen Bolzano, January February 2015

Edited by

Marco Baratieri, Vincenzo Corrado,
Andrea Gasparella, Francesco Patuzzi

bu,press

bozen
bolzano
university
press

Graphic and parametric tools for preliminary design stage of natural ventilation systems

Margherita Ferrucci – Université Paris-Est, IUAV University of Venice – marferit@gmail.com

Maurizio Brocato – ENSA Paris-Malaquais – maurizio.brocato@mac.com

Fabio Peron – IUAV University of Venice – fperon@iuav.it

Francesca Cappelletti – IUAV University of Venice – francesca.cappelletti@iuav.it

Abstract

In this paper we developed a simplified graphical visualization to provide a preliminary understanding of aerodynamic pressure distributions around tall buildings and to estimate the best positions for ventilation openings. This graphical model is based on a database of pressure coefficients hold by parametrical two-dimensional CFD (Computational Fluid Dynamics) simulations over several rectangular shape profiles. The pressure values are obtained by CFD simulations of a stationary flow (High Reynolds), with a K-epsilon turbulence model coupled with Navier-Stokes equations, by using Finite Elements Methods. Whilst turbulence model is well-known, the innovative application is the parameterization of the CFD simulations. The parameters considered here are the ratio between length and width of a rectangular shape and the wind direction (degrees azimuth). Our model adapts automatically to different shapes and various wind directions. Though not able to capture the same level of detail as the three-dimensional CFD simulations or experimental tests, it provides a rapid and intuitive guidance for architects at the preliminary design stage of a natural ventilation system. The final graphical visualizations, together with some simple recommendations, can be exploited by designers having no knowledge in aerodynamics.

1. Introduction

1.1 Airflow around buildings

The use of natural ventilation as a passive strategy for cooling needs reduction has been largely discussed by many authors, since free and mechanical ventilation can reduce the plant capacity and the energy consumption in air-

conditioned buildings. Moreover, the use of airflow to remove indoor pollutants and to guarantee a good indoor thermal environment is quality is probably the most recognized advantage of natural ventilation. Mochida (Mochida et al. 2005) demonstrated that wind-driven natural ventilation is an effective way to maintain a comfortable and healthy indoor environment, as well as offering an energy-saving alternative to mechanical ventilation, even though its effectiveness, for a given climatic condition, is strongly affected by the position of the openings on the facades. In fact, natural ventilation, infiltration and exfiltration are affected by wind, causing variable surface pressures on envelope buildings.

The major efficacy of natural ventilation in removing pollutant is achieved when the air flows through an indoor space, determining the so-called cross-ventilation. Cross-ventilation depends on the impact of the wind over the building envelope, which produces a variable pressure field (positive and negative). This pressure difference is the driving force for the airflow through the building. So the effectiveness of wind-driven ventilation depends on the external wind conditions and on the building design (Etheridge et al., 1996).

In a tropical humid climate, for example, the speed of the airflow is used to improve the thermal comfort. Consequently, to obtain cross-ventilation, buildings are designed by choosing their location, orientation, shape, window positions and the internal partitions (Gandemer J.,1992, Olgyay V.,1973).

On the other hand, stack ventilation is driven by the difference between outdoor and indoor air density, caused by temperature difference. Also in

this case, the direction and velocity of the wind and the shape of the building affect the system. (Katarzyna Gładyszewska-Fiedoruk et al. 2012). Consequently, it is impossible to dissociate the design of the shape of a building from the ventilation systems (either natural or mechanical). The pressure distributions expressed by the pressure coefficients, caused by the flow around the building, plays an important role at the beginning stages of design.

1.2 The pressure coefficients

Wind pressure distributions are described by pressure coefficients

$$C_p = \frac{P_s - P_o}{P_d} \text{ with } P_d = \frac{\rho U_h^2}{2}$$

where P_s is the static pressure at a given point on the building facade, P_o is the static reference pressure, P_d is the dynamic pressure (the pressure is expressed in Pascal units), ρ is the air density (kg/m^3) and U_h is the wind speed of undisturbed flow (m/s).

Pressure coefficients can be obtained by full-scale tests, wind tunnel tests, fluid dynamic simulations, parametric equations and databases derived from measurements. The first three methods are more accurate than the parametric equations, even though, being based on non-parametric methods, it is not possible to transpose the obtained results to other different cases.

These studies are focalized on a geometry with only few wind directions. Moreover, they are expensive, time consuming, and they require consequential time and expertise. In addition, these methods are out of reach for architects and designers who, in the early stages of their project, need to visualize the pressure distributions to choose the opening positions and the best orientation of the building.

The most popular parametric equation for low-rise buildings is that of Swami and Chandra (Swami et al. 1987), used also in the ASHRAE guidelines (ASHRAE 2001). Other authors, Grosso (Grosso M.,1992.) and Eldin (Eldin AS. 2007) expand this work to include the effects of shielded environment. Recently, Patrizi and Muehleisen (Muehleisen R. T. et al. 2013) developed a

parametric equation derived on the Tokyo database. An interesting review of several equations and methodologies was provided by Cóstola (Cóstola et al. 2009). This research proves that the pressure coefficients on building facades are influenced by a wide range of parameters, so that it is practically impossible to take into account the full complexity of the C_p variation. Every method gives the surface-averaged wind pressure coefficients on the facade for each side of a low-rise parallelepiped (or cubic) building, with variable depth-to-breadth short-side and depth-to-height ratios, and for variable wind angle direction. For a non-expert user, to collect the pressure coefficients is not as immediate as knowing their spatial variation, because there does not exist a quick and simple approach to estimate the C_p positions.

1.3 Aim of the study

In this paper a simplified graphical visualization has been developed to provide a preliminary understanding of aerodynamic pressure distributions around rectangular shapes. The same computation methodology and post-data processing can be easily applied to different 2D geometries. The 2D fluid dynamic simulations over the profiles corresponds to the cross-section 3D fluid dynamic simulations over an infinitely long body. Due to the fact that this tool is addressed to architects and designers for the preliminary conception of a ventilation opening system integrated in a building, we make the assumption that the results around a 2D shape can be transposed to a cross section of a tall building in an area not influenced by the ground and the roof. Our results, though not reliable if applied to the whole building, give the tendencies of pressure distributions on a cross section. It is important to note that our study concerns only one aspect of the design process, namely, the best location of openings.

2. Method

The geometry considered here is a rectangular shape of width W and height H , located in a canal

(height: 14 m; length: 20,5 m). The ratio r between H and W is variable and the perimeter P is taken constantly equal to 4 m. So the edge lengths change on the basis of their aspect ratio r . The values of the ratio chosen for the analysis are

$$r = \{1/n, n\} \text{ with } n=1, \dots, 8$$

which are the most commonly used for the cross section of buildings. In this way it is possible to cover a wide range of building typologies. The geometry is therefore identified only with one parameter, i.e. the aspect ratio r (Fig. 6).

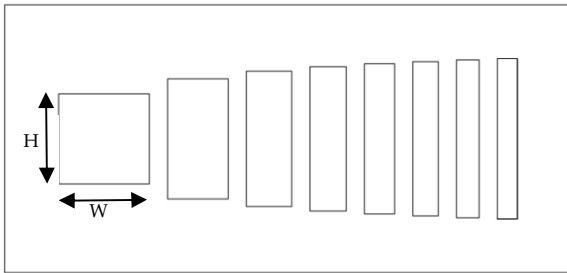


Fig. 6 – Shapes with variable ratios $r=\{1,2,3,4,5,6,7,8\}$ in this order

The model was studied as it was located towards different wind directions determining different incidence angles of the wind stream over the building facades. The wind directions considered for the study have the following azimuth:

$$\alpha = \{0^\circ, 10^\circ, 20^\circ, 30^\circ, 40^\circ, 45^\circ\}.$$

The wind direction has been simulated pivoting the rectangle around its centroid (Fig. 7). A counterclockwise pivoting corresponds to a positive wind azimuth. The reduced azimuth range (from 0° to 45°), coupled with the double symmetry of the rectangular shape (along the middle x -axis and the middle y -axis), gives the possibility to investigate the pressure field for all degrees from 0° to 350° . Combining the azimuth angles with the different aspect ratios, a total of 90 cases has been computed.

2.1 Simulations

A database of pressure coefficients has been computed by means of parametrical two-dimensional CFD simulations over all the 90 cases. The geometry, the meshing generation and the computational simulations have been performed in Cast3M environment, a computer code used

mainly in the analysis of structures by Finite Elements Methods and also for CFD simulations. Thanks to this software we can launch a series of simulations adapting the mesh to the geometry. The flow domain is split into a structured grid with quadrilateral meshes. The domain contains around 5000 elements (the number of elements is variable with the aspect ratio). The mesh is fined progressively near the rectangle (Fig.2).

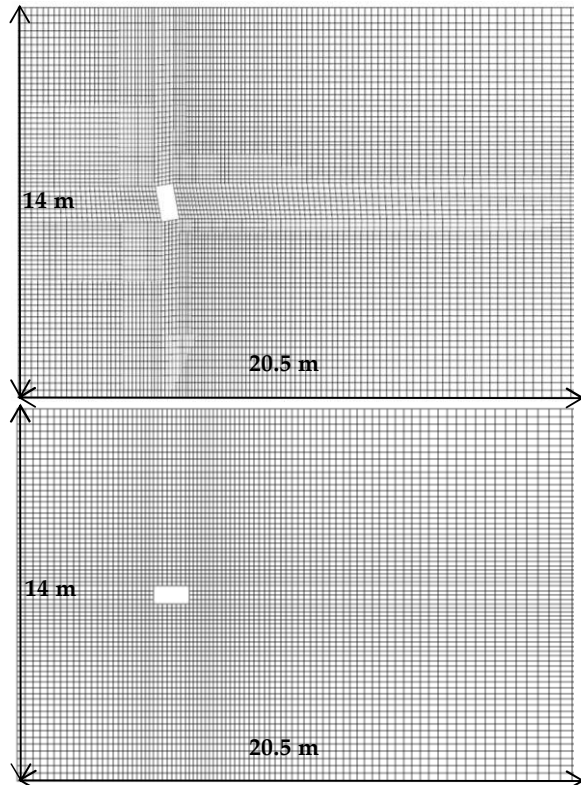


Fig. 7 – Mesh grid of the rectangle in the canal; up: $r = 2, \alpha = 10^\circ$; down: $r = 0.5, \alpha = 0^\circ$

The pressure values have been obtained by CFD simulations of a stationary airflow (High Reynolds, $Re = 5.5 \cdot 10^5$, with kinematic viscosity equal to $15.6 \cdot 10^{-6} \text{m}^2/\text{s}$) with the standard K-epsilon turbulence model coupled with Navier-Stokes equations by using Finite Elements Methods. The wall-law is applied on each side of the rectangle. The flow has a uniform velocity on the inlet (right of the canal), with only the horizontal component. Whilst the turbulence model is well-known, the innovative application is the parameterization of a CFD simulation. The parameters considered are the aspect ratio of the rectangular shape and the wind

direction. The model is able to adapt automatically to different shapes and various wind directions.

2.2 Data processing

The data processing of the pressure coefficients and the resulting graphical visualizations have been developed within Wolfram Mathematica®. The pressure coefficients are plotted along the development line of the rectangle, whose length corresponds to the perimeter $P = 4$ m. However, to compare all sides of every shape in the same graphic, we scaled the dimension of each edge to its maximum length. In this way, rectangles with edges of different length can be plotted in the same graph. With these assumptions, it is possible to compare the pressure coefficients and their positions for rectangles with edges of different length and different aspect ratio. This operation was applied to each case study. The rectangle sides have been enumerated in the following way: 1 for the windward side, 3 for the leeward side, 2 for the underside and 4 for the upper side.

We present here three types of visualizations (for a reduced number of study cases): Fig.3 and Fig.5 show the evolution of pressure coefficients over the shape for the different aspect ratios when the latter varies, whereas Fig.6 shows the evolution of pressure coefficient for different azimuth angles and a fixed aspect ratio. The pressure distribution around the scaled rectangles is shown in Fig. 8, and the pressure distribution along the contour in Fig. 5 and Fig. 6.

In Fig. 5 and Fig. 6 the pressure coefficients (C_p) are in the y -axis and their position in the x -axis (contour perimeter). The rectangular side 1 is represented between the abscissa 0 and 1, side 2 between 1 and 2, side 3 between 2 and 3, and side 4 between 3 and 4. The total length of the contour is the same for every rectangle. To simplify the comprehension in Fig. 5, the lines representing the rectangles with $r = \{ 1, 2, 4, 8, 1/2, 1/4, 1/8\}$ are thicker than the others. The line corresponding to $r=1$ is always a red line.

In the second representation (Fig. 3) the C_p 's are plotted around a square. The square represents simultaneously the scaled rectangles in order to compare the C_p 's and their positions for rectangles

with edges of different length and different ratio. The positive values are inside the shape, the negative ones outside. The shape orientation is the same for the CFD simulation: the windward side (side 1) on the left, the leeward side (side 3) on the right. For a better visualization, we represented the computations for a small choice of the ratios: $r = \{ 1, 2, 4, 8, 1/2, 1/4, 1/8\}$.

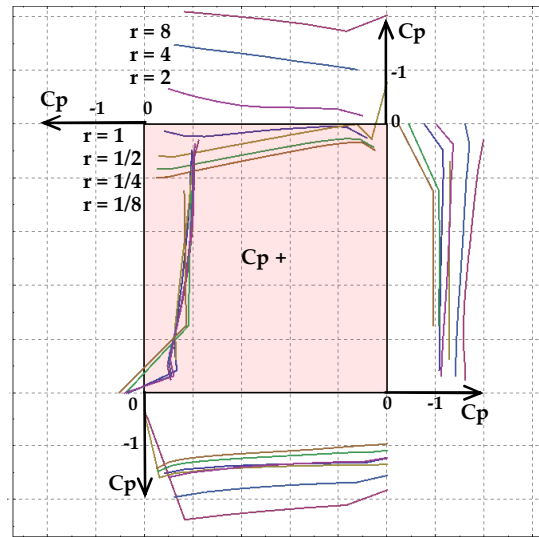


Fig. 8 – Pressure coefficient (C_p) distribution for azimuth $\alpha = 30^\circ$.

At a later stage, a fourth data processing is performed to extrapolate more information about the pressure difference potential. For an upwind point A and a downwind point B, the pressure difference can be taken as an indicator of the force driving the internal flow, with unique openings in A and B.

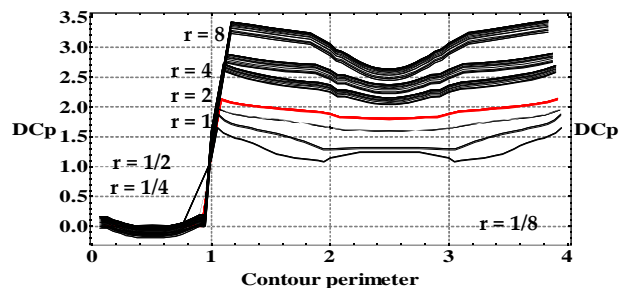


Fig. 9 – Pressure coefficient difference (DC_p) for azimuth $\alpha = 0^\circ$

The obtained results are displayed in Fig. 9: the difference between pressure coefficients (DC_p) at two different points of the contour perimeter is represented in the y -axis and its position in the x -axis (the DC_p 's computed with respect to upwind

points of side 1 is plotted against the downwind points of side 2, 3 and 4). For each aspect ratio r , coupled with a particular wind azimuth α , we get a line passing through each point of side 1. Therefore, the number of lines increases with the value of r .

3. Discussion

Thanks to this graphic giving the pressure coefficient distribution, architects may optimize the ventilation system of a project by choosing the opening positions that maximize the pressure difference. Similarly, they are able to understand which side, or part of it, is in a low/high pressure area. We note here that in this work we focus on the external flow without considering the internal flow paths and their losses.

The graphics of pressure coefficient distribution (Fig. 9, Fig. 5 and Fig. 6) are helpful for the preliminary design. For instance, they show when sides 1 and 4 have positive or negative pressure and the corresponding value. For example, the pressure on side 4 (rectangles with $r = 1$) becomes positive for azimuths $> 30^\circ$. Therefore, for a tall building with $r = 1$ situated in an open environment, the openings on sides 1 and 4 will be inlet openings when the azimuth wind is around 30° .

With the graphic typology of Fig. 5, architects can apply the pressure coefficients on the perimeter of a cross section of a tall building which is already oriented. In this way, they can evaluate the best aspect ratio to have a specific pressure distribution; they may also choose the position of the openings for a cross ventilation by reading the opening positions on the x -axis. Similarly, using the Fig. 6, they can estimate the best building position to develop a good cross ventilation with a fixed aspect ratio.

With some more data processing, it is possible to visualize the pressure difference between a point on side 1 (windward) and all the other points.

As the long edge is on the windward side, the ventilation potential increases, since this maximizes the pressure differences between the opposite sides. Therefore, for a high ventilation

potential, the solutions are those with the aspect ratio $r > 1$. Fig. 9 shows that the pressure difference increases with the aspect ratio. This happens for every azimuth until 45° , then the trend reverses. The smallest possible variation between minimum and maximum DC_p 's is the rectangle with $r = 1$ (the square). The maximum DC_p is 3.4 and it occurs with $r = 8$, the minimum is 1.1 with $r = 1/8$. As an example, with a dynamic pressure of 15 Pa (wind velocity 5 m/s and air volumetric mass density equal to 1,2 Kg/m³), we obtain a maximum pressure difference of 51 Pa and a minimum pressure difference of 16.5 Pa.

There are pressure discontinuities on the edges caused by vortex detaching: in Fig. 9, Fig. 10 and Fig. 6 the jumps of the plotted functions corresponds to these edges. For a wind azimuth $\alpha = 0^\circ$, the maximum values of DC_p are near the edges.

4. Conclusions

Our graphic tools provide a rapid and intuitive guidance for architects at the preliminary design stage of a natural ventilation system.

An original application is the parameterization of CFD airflow building simulation. In fact, though the use of parametric design in architecture is well known, the CFD parametric studies are developed mostly in aerodynamics (aerospace and aeronautic engineering).

This method can be efficiently applied to simple two-dimensional objects, in particular for rectangular shapes (defined by their aspect ratio, r), which can be identified to cross sections of a standard building. Since the pressure coefficients for rectangles are well known in scientific literature, we can easily verify our results.

By a specific data processing we compare the pressure coefficients and the pressure coefficient difference for every rectangle with different aspect ratio. Therefore, we provided three different types of graphic giving the pressure coefficient distribution around the rectangles (Fig. 8, Fig. 5 and Fig. 6) and the pressure difference potential (Fig. 4). The latter can be taken as an indicator of the force driving the internal flow.

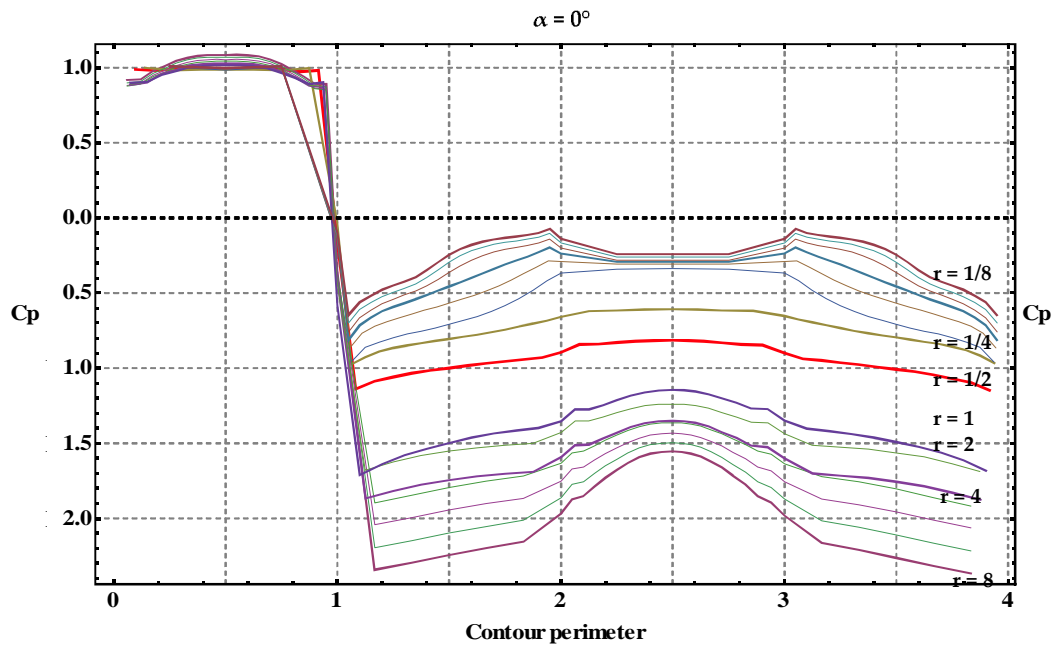


Fig. 10 – Pressure coefficient (C_p) along the contour for $\alpha = 0^\circ$

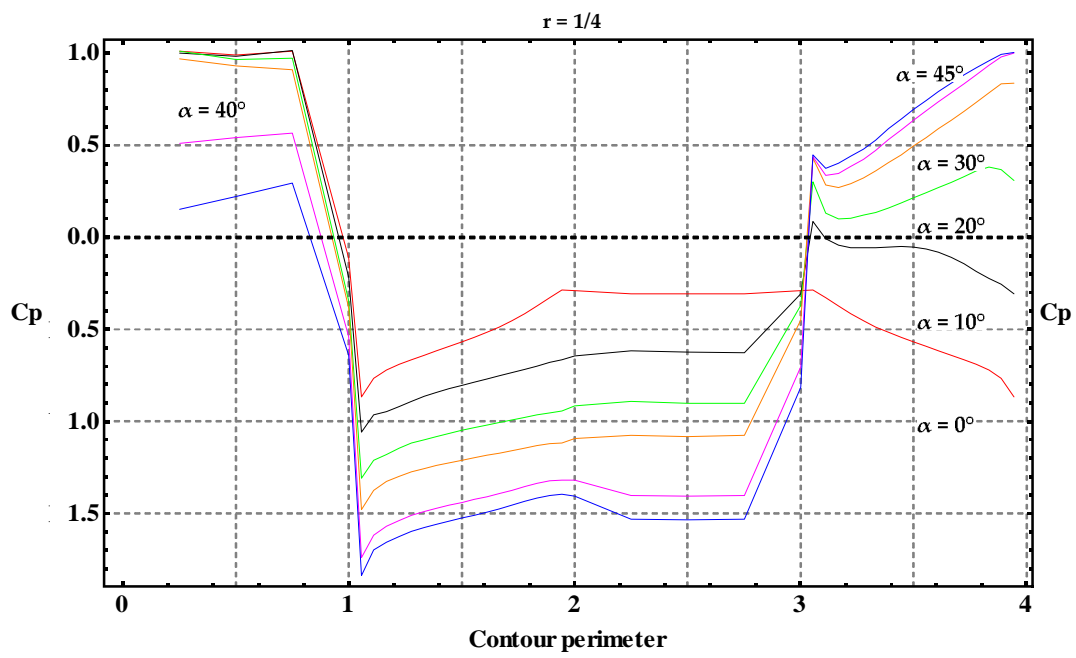


Fig. 11 – Pressure coefficient (C_p) along the contour for $r = 1/4$

5. Acknowledgement

The first author is partially supported by *Université Franco Italienne* and *Paris-Est University*. The authors wish to thank the «*Commissariat français à l'Énergie Atomique et aux énergies alternatives (CEA)*» for making Cast3M freely available.

6. Nomenclature

Symbols

H	height (m)
W	width (m)
P	perimeter (m)
r	length/width (aspect ratio)
α	azimuth angle (°)
C_p	pressure coefficient
DC_p	pressure coefficient difference

References

Journal papers

- Cóstola D., Blocken B., Hensen J.L.M.. 2009. "Overview of pressure coefficient data in building energy simulation and airflow network programs." *Building and Environment* 44: 2027–2036.
- Eldin AS. 2007. "A parametric model for predicting wind-induced pressures on low-rise vertical surfaces in shielded environments." *Solar Energy* 2007: 81:52–61.
- Grosso M. 1992. "Wind pressure distribution around buildings: a parametrical mode." *Energy and Buildings* 18:101–31.
- Katarzyna Gładyszewska-Fiedoruk, Andrzej Gajewski. 2012. "Effect of wind on stack ventilation performance." *Energy and Buildings* 51: 242–247.
- Mochida A., Yoshino H., Takeda T., Kakegawa T., Miyauchi S. 2005. "Methods for controlling airflow in and around a building under cross ventilation to improve indoor thermal comfort." *Journal of Wind Engineering and Industrial Aerodynamics* 93 (2005) 437–449.
- Muehleisen R. T., Patrizi S. 2013. "A new parametric equation for the wind pressure

coefficient for low-rise buildings." *Energy and Buildings* 57: 245–249.

- Swami MV, Chandra S.1988. "Correlations for pressure distribution on buildings and calculation of natural-ventilation airflow." *ASHRAE Transactions* 94: 243–66.
- Swami MV, Chandra S. 1987. "Procedures for calculating natural ventilation airflow rates in buildings-Final report FSEC-CR-163-86." *Cape Canaveral: Florida Solar Energy Center*.

Books

- ASHRAE. ASHRAE handbook – fundamentals. Atlanta: ASHRAE; 2001.
- Etheridge D., Sandberg M. 1996. *Building Ventilation: Theory and Measurement*. John Wiley and Sons.
- Gandemer. 1992. *Guide sur la climatisation naturelle de l'habitat en climat tropical humide, Tome 1: Méthodologie de prise en compte des paramètres climatiques dans l'habitat et conseils pratiques*. CSTB, Nantes, pp. 64–68.
- Olgay V. 1973. *Design with Climate: Bio-climatic Approach to Architecture Regionalism*, Princeton University Press, Princeton, NJ, USA pp.94–112.

Online resource

- Tokyo Polytechnic University, Aerodynamic Database of Low-Rise Buildings, <http://www.wind.arch.t-Kougei.ac.jp/system/eng/contents/code/tpu>